Applied Soft Computing Journal xxx (xxxx) xxx

Contents lists available at ScienceDirect

Applied Soft Computing Journal

journal homepage: www.elsevier.com/locate/asoc

OCE-NGC: A neutrosophic graph cut algorithm using optimized clustering estimation algorithm for dermoscopic skin lesion segmentation

Ahmed Refaat Hawas [a], Yanhui Guo [b], Chunlai Du [c], Kemal Polat [d,*], Amira S. Ashour [a]

[a] Department of Electronics and Electrical Communications Engineering, Faculty of Engineering, Tanta University, Tanta, Egypt
[b] Department of Computer Science, University of Illinois at Springfield, Springfield, IL 62703, USA
[c] School of Computer, North China University of Technology, Beijing, China
[d] Department of Electrical and Electronics Engineering, Faculty of Engineering and Architecture, Bolu Abant Izzet Baysal University, 14280 Bolu, Turkey

ARTICLE INFO

Article history:
Received 1 July 2018
Received in revised form 2 November 2019
Accepted 6 November 2019
Available online xxxx

Keywords:
Dermoscopic images
Skin lesion
Genetic algorithm
Neutrosophic c-means
Neutrosophic graph cut

ABSTRACT

Automated skin lesion segmentation is one of the most crucial stages in dermoscopic images based diagnosis. To guarantee efficient unsupervised clustering-based segmentation, a histogram-based clustering estimation (HBCE) algorithm can be used to obtain the initial number of clusters with their corresponding centroids. Accordingly, the present work introduced a novel skin lesion segmentation algorithm, called optimized clustering estimation for neutrosophic graph cut algorithm (OCE-NGC). Firstly, the genetic algorithm (GA) is used to optimize the HBCE procedure by finding its optimal threshold values which are functions of a factor, called β to be optimized. This optimization process guarantees the optimal determination of the initial number of clusters and their corresponding centroids for further use in the proposed clustering process. Thus, the skin lesion dermoscopic images are then mapped into the neutrosophic set (NS) domain which is computed by the neutrosophic c-means (NCM). The NCM groups the pixels in the dermoscopic images using the pre-determined optimal number of clusters obtained by the optimized HBCE. Finally, a cost function of the graph cut (GC) algorithm is defined in the NS domain for the segmentation process. The experimental results established the superiority of the proposed OCE-NGC approach in comparison with the traditional HBCE with NCM only, the traditional HBCE with the NGC, and the typical GC. In a public dataset, the proposed approach achieved 97.12% and 86.28% average accuracy and average Jaccard (JAC) values, respectively.

© 2019 Elsevier B.V. All rights reserved.

1. Introduction

Abnormalities/lesions are the main clinical signs for several skin diseases, such as melanoma, chickenpox [1]. Their early detection and diagnosis might guarantee successful treatment planning. However, this process is complex and error-prone for the inexpert dermatologists using the traditional methods. Subsequently, automated skin lesion regions detection attracted researchers developing computer-aided diagnosis systems (CADs). In dermoscopy images, the automated lesion detection is considered a challenging task owing to some limitations, including the artifacts (e.g. air bubbles, hairs, and skin lines), low contrast between the surrounding skin and the lesion, multicolored regions inside the lesion, and the fuzzy/irregular lesion borders.

Various studies have been established for lesion/border detection in the dermoscopic skin lesion images using the lesions clinical features, including abrupt border cutoff, border irregularity, asymmetry of the lesion's border, blue–white areas of the lesion, atypical pigment networks, and globules. For skin lesion image segmentation, Rajab et al. [2] conducted a comparative study between the region-based segmentation using optimal threshold method and the neural network edge detection method. Automated segmentation in dermoscopy images has been implemented by Wang et al. [3] based on an improved watershed algorithm and the neural network classifier.

Furthermore, clustering-based approaches have a significant role in pattern recognition and numerous engineering applications [4,5]. These approaches capture the images' global characteristics by computing the texture or color features from the image to professionally segregate the data. Typically, the

* Corresponding author.
E-mail addresses: ahmed.hawas@f-eng.tanta.edu.eg (A.R. Hawas), yguo56@uis.edu (Y. Guo), duchunlai@ncut.edu.cn (C. Du), kpolat@ibu.edu.tr (K. Polat), amira.salah@f-eng.tanta.edu.eg, amirasashour@yahoo.com (A.S. Ashour).

https://doi.org/10.1016/j.asoc.2019.105931
1568-4946/© 2019 Elsevier B.V. All rights reserved.

clustering algorithms can be categorized into hard clustering approaches, which group each data point to only one specific cluster, and soft clustering approaches, which specify each data point to different clusters with different degrees of membership [6]. The main advantages of the hard segmentation approaches, such as the k-means, are their fast speed and simplicity. Nevertheless, the hard segmentation approaches minimize the intra-cluster variance without considering the global minimum of variance, as well as the number of clusters, should be assumed initially which might lead to poor clustering results [7]. To resolve such limitations, the soft clustering procedures can be applied, where the fuzzy c-means algorithm (FCM) is considered one of the most prevalent algorithms for segmentation. An iterative minimization of a cost function is performed to obtain the data's membership degrees in the FCM [8]. Due to the fuzzy/irregular lesion borders in the dermoscopic images, fuzzy set theory has been employed is numerous segmentation to deal with such uncertainty. Zhou et al. [9] employed a fuzzy c-means (FCM) approach and an anisotropic mean shift algorithm for dermoscopic images segmentation. Lee and Chen [10] used the FCM clustering for skin lesion segmentation based on type-2 fuzzy sets method. However, the FCM has several drawbacks, including its sensitivity to the noise and its dependence on the initial number of clusters and centroid settings [11]. To overcome both the FCM's sensitivity to noise, and the indeterminate information in the dermoscopic images, different studies have been conducted using the neutrosophic set (NS). Guo et al. [12] applied a skin lesion detection approach based on the neutrosophic clustering and adaptive region growing algorithms. The Shearlet transform has been mapped the dermoscopic images into the NS domain using three membership functions, namely true, indeterminate, and false memberships. A neutrosophic c-means (NCM) clustering algorithm has been used to segment the dermoscopic images. Ashour et al. [13] realized a novel skin lesion detection scheme based on the genetic algorithm (GA) based optimized NS to reduce the indeterminacy in the dermoscopic images. Afterward, a k-means clustering procedure has been used to segment the skin lesion regions.

Since the clustering is an unsupervised learning process, it requires prior setting to the used number of clusters and centroids. Various studies have been conducted to determine the optimal number of clusters [14–17]. Ashour et al. [18] developed a histogram-based clustering estimation (HBCE) algorithm to define the required number of clusters in the NCM clustering procedure for skin lesion detection in the dermoscopy images from the public dataset. A peak search method has been applied to the histogram of the dermoscopic image to record the local and global maximum values.

Apart from these segmentation techniques, the graph-based approaches arisen as high-quality valuable tools for energy minimization problems. These graph-based segmentation approaches establish an imperative image segmentation method and have been effectively applied to a broad range of segmentation problems [19,20]. Lézoray et al. [21] extracted the skin lesion in multispectral dermoscopy images by segmenting the images with a graph-based method after hairs removal. Flores et al. [22] generated a dictionary using a modified information-theoretic dictionary learning (ITDL) method to represent the skin image patches. Afterward, normalized graph cuts partitioned the set of projected patches in healthy or unhealthy regions. For melanoma identification, Kéchichian et al. [23] proposed a graph-cut image segmentation model based on the probabilities learned by a support vector machine (SVM) classification process using the color, shape and texture information. Guo et al. [24] implemented a neutrosophic graph cut (NGC) for image segmentation, where the image was mapped in the NS domain followed by indeterminacy filtering operation. Afterward, a maximum-flow algorithm on the GC was defined on the image and the weight for each pixel was introduced after the indeterminacy filtering process. The results established the efficiency of the NGC approach.

Since the dermoscopic lesion images have complicated characteristics, including the irregular/fuzzy lesion's border shape, low contrast transition between the normal skin regions and the lesion ones, the presence of some artifacts, such as the hair, air bubbles, multi-colored skin lesion interior, and dissimilar lesion types, hybrid segmentation techniques have been involved to handle such complex segmentation problem, and have become a perceptible evolving direction for efficient segmentation and achieved optimal segmentation results [25,26]. Consequently, the present work has the intention to improve the segmentation accuracy by gaining the benefits of both the clustering-based segmentation and the graph-based segmentation by combining both the NCM and the GC techniques together to achieve the fast, unsupervised, and efficient solution for the skin lesion segmentation task. Furthermore, to resolve the drawback of the required proper determination of the number of clusters in the NCM, in the current work, the HBCE algorithm [18] is optimized to determine the optimal number of clusters and their centroids. Finally, the optimal results are used in the neutrosophic graph cut (NGC) for the dermoscopic images segmentation where the NCM clustering is integrated within the GC approach. This proposed OCE-NGC approach improved the segmentation overall performance compared to the used method in [18] and segmented the failed cases in [18] accurately.

The structure of the following sections in the present work is ordered as follows. Section 2 introduces the GA-based optimization to determine the optimal number of clusters, reviews the NCM clustering, the typical GC framework, and NGC algorithm with along with illustrating the proposed dermoscopic images segmentation system. The experimental results and discussion are presented in Section 3. Lastly, Section 4 concludes the proposed work.

2. Methodology

A clustering-based segmentation has a significant role in image processing applications. However, it is a challenging issue to select the number of clusters and initialize their centroids accurately. With inaccurate initialization of the number of clusters or their corresponding centroids, the clustering-based segmentation approaches may stuck into local minima and not produce an optimal solution, increase the iterations time/computation cost, and lead to the inaccurate segmentation process. To resolve these limitations, the proposed work proposes a GA based HBCE algorithm to determinate the number of clusters and their centroids for NCM, and then they are used in the neutrosophic graph cut (NGC) for the skin lesion dermoscopic images segmentation.

2.1. Optimized clusters number determination

The key factors that influence the clustering performance are the number of clusters and the initial cluster centroids, which generally are assumed by the users of clustering algorithms or randomly selected. Automated and adaptive identification of the cluster numbers becomes essential [27,28] to improve the performance of the clustering algorithm. For automated image segmentation, the number of clusters has to be identified before clustering. Typically, the histogram of an image defines the frequency distribution of its intensity levels and characterizes the number of pixels at each intensity level in the image, and can be used to roughly identify clusters and improve the clustering performance.

Please cite this article as: A.R. Hawas, Y. Guo, C. Du et al., OCE-NGC: A neutrosophic graph cut algorithm using optimized clustering estimation algorithm for dermoscopic skin lesion segmentation, Applied Soft Computing Journal (2019) 105931, https://doi.org/10.1016/j.asoc.2019.105931.

In the present work, the histogram-based clustering estimation (HBCE) algorithm [18] is applied. Typically, the histogram shows the number of occurrences of each intensity value. On the histogram, peaks and pits are local maximum and minimum, respectively. Generally, in the histogram, a point is considered as a peak point if its intensity value is larger than its forward and afterward neighboring points. A point is recorded a pit (valley) point if it has the least intensity value compared to its forward and afterward neighbors, which can be expressed as follows for a point p:

$$Peak = \{p \,|H(p-1) < H(p) \&\& H(p) > H(p+1)\} \tag{1}$$

$$Pit = \{p \,|H(p-1) > H(p) \&\& H(p) < H(p+1)\} \tag{2}$$

where H is the histogram in the image. Thus, by screening the histogram, the peaks and their following pit (valley) points are determined, and the location of the peak and pit points is also recorded as:

$$PeakPitVector_{\text{intensity}} = [PKL_1, PTL_1, PKL_2, PTL_2, \ldots, PKL_i, PTL_i, ..] \tag{3}$$

The accuracy of HBCE algorithm in the present work for determining the accurate number of clusters depends mainly on two sequential procedures, namely intensity-search based procedure, and frequency-search based procedure.

In the *intensity-search based* procedure, the distance between the gray levels of two consecutive points on the *PeakPitVector* is calculated which represents the distance in gray level intensity value of peak and valley points. Thus, the *LD* is a vector consists of the distance values on the histogram for different *i*.

$$LD(i) = |PKL(i) - PTL(i)| \tag{4}$$

where $PKL(i)$ and $PTL(i)$ are the gray intensity level values of the ith peak and pit, respectively. In addition, the mean of the distance vector is expressed as follows:

$$\overline{LD} = mean(LD(i)) \tag{5}$$

Then, the intensity threshold $Th_{\text{intensity}}$ is calculated by multiplying the mean distance *LD* with the parameter $\beta_{\text{intensity}}$ as follows:

$$Th_{\text{intensity}} = \overline{LD} * \beta_{\text{intensity}} \tag{6}$$

where $\beta_{\text{intensity}}$ is the first parameter of the factor β to be optimized using GA to find its optimal value.

From the intensity search based procedure, an intensity threshold value is calculated, which is used to scan the $PeakPitVector_{\text{intensity}}$ values and consider every horizontal distance greater than this threshold in the next frequency search based procedure. Hence, the $PeakPitVector_{\text{intensity}}$ is smoothed by keeping only the points (gray intensity level) that have a corresponding horizontal distance are greater than the intensity threshold $Th_{\text{intensity}}$ in a generated *SLD* vector.

$$SLD[i] = PeakPitVector_{Intensity}[i] > Th_{\text{intensity}} \tag{7}$$

Then, this *SLD* is fed to the frequency-based search procedure to determine the final number of clusters and its corresponding centroids.

In the *frequency-search based* procedure, the difference between the height values (which refers to the frequency (number of occurrences) of the corresponding level intensity) of the gray intensity levels existing in the *SLD* vector is defined as:

$$HD(i) = |SLD(PKL(i)) - SLD(PTL(i))| \tag{8}$$

Furthermore, the mean of the height distance vector's values is expressed as follows:

$$\overline{HD} = mean(HD(i)) \tag{9}$$

Another threshold is calculated using the following formula:

$$Th_{frequency} = \overline{HD} * \beta_{frequency} \tag{10}$$

where $\beta_{frequency}$ is the second parameter of factor β that will be optimized using GA. to find the optimal value that will generate an accurate number of clusters.

Hence, the final smoothed $PeakPitVector_{\text{intensity}}$ is obtained by reducing the size of the distance vector *HD* and keeping only the points that have a corresponding distance greater than $Th_{frequency}$ to generate the smoothed *SHD* vector.

$$SHD[i] = SLD[i] > Th_{frequency} \tag{11}$$

Finally, the number of clusters in an image is equal to the size of the *SHD* vector, which can be formulated as follows:

$$N_c = number\ of\ attributes\ \text{in}\ SHD \tag{12}$$

where N_c refers to the number of clusters. Furthermore, the centroid of each corresponding cluster is defined from the histogram level of the corresponding cluster point, which can be formulated as:

$$CC = [CC_1, CC_2, \ldots, CC_i, \ldots] \tag{13}$$

where *CC* includes the corresponding histogram level value at each cluster and CC_i refers to the centroid of the ith cluster. These previous procedures for estimating the number of clusters and their centroids depend on the threshold values, namely $Th_{\text{intensity}}$ and $Th_{frequency}$, which are used to retain the candidate peaks and pits during the search processes. Each threshold value consist of two terms, the first term is the mean of the distances, which is image-dependent, and the second term includes a factor parameter $\beta_{\text{intensity}}$ in $Th_{\text{intensity}}$ and $\beta_{frequency}$ in $Th_{frequency}$, which are used to adjust the threshold value and are independent on the image.

According to the image histogram, the intensity–frequency (I–F) based HBCE algorithm is employed to define the number of clusters and the corresponding centroids. Algorithm 1 illustrates the steps of the I–F based HBCE approach.

In the above algorithm, the intensity-search refers to the use of the intensity level of the histogram to determine the peaks and the pits, while the frequency-search based refers to the use of the frequency of occurrences in the histogram level. Using these procedures sequentially reduces the informative points in the histogram to the estimated number of clusters, then the centroids of the corresponding clusters are determined according to the histogram level at the determined centroid in the final reduced in size vector *SHD*.

In the present work, since a global search can be provided by using the GA in the design space, the GA is used in the present work to optimize the HBCE parameters. This advantage of the GA guarantees its ability to avoid being trapped in local optima, which occurs when using the Gradient-based methods. Furthermore, the GA has the ability to deal with non-analytic functions, where it does not require derivative information during its procedure. Compared to the evolutionary algorithms (EA), the GA uses both the crossover and mutation operators that makes it the most popular optimization method with efficient diverse.

Thus, the proposed approach applied the GA for optimization to find the optimal value of $\beta_{\text{intensity}}$ and $\beta_{frequency}$, denoted as $\beta_{\text{intensity}-optimal}$ and $\beta_{frequency-optimal}$, respectively. These optimal values are the main parameters in the threshold values in the HBCE algorithm. During the GA optimization process, there are three main operators, selection, crossover, and mutation. It starts with a set of solutions (population) and engages the solutions from one population to yield a new population for finding better population. The solutions are designated to produce new solutions (offspring) based on the determined fitness function. The superior solutions having superior fitness will remain in the next

Please cite this article as: A.R. Hawas, Y. Guo, C. Du et al., OCE-NGC: A neutrosophic graph cut algorithm using optimized clustering estimation algorithm for dermoscopic skin lesion segmentation, Applied Soft Computing Journal (2019) 105931, https://doi.org/10.1016/j.asoc.2019.105931.

Algorithm 1: I-F based HBCE approach

Start

Calculate the histogram of the image

Find the number of clusters and their corresponding centroids by performing two sequential processes one using the ***intensity-search based*** procedure and then use the ***frequency-search based***

First Histogram smoothness using the *intensity-search based* procedure:

Apply the ***intensity-search based*** by searching all histogram intensity levels to find the peaks and pits point procedure

Construct the vector of the peak and pit points ($PeakPitVector_{\text{int}ensity}$)

Build a new vector LD that contains the distance between two successive points in the vector

Calculate the mean of the measured distances and generate $\overline{LD}$

Determine the threshold $Th_{\text{int}ensity}$ to generate the SLD vector to smooth the histogram by keeping only the points that have a corresponding distance greater than $Th_{\text{int}ensity}$

Second Histogram smoothness using the *frequency-search based procedure*:

Perform the second smoothness on SLD by using the ***frequency-search based*** procedure

Build a new vector HD that contains the distance between two successive points in the SLD vector by finding the difference between the frequency of the histogram level

Calculate the mean of the measured height difference and generate $\overline{HD}$

Determine the threshold $Th_{frequency}$ to generate the SHD vector to smooth the histogram by keeping only the points that have a corresponding distance greater than $Th_{frequency}$

Determine the final number of clusters

Determine each cluster centroid

End

Algorithm 2: Genetic Algorithm Procedure

Produce *n* random populations

Compute the average Dice of the images in the training set as the fitness function

Generate a new population using the GA operations, namely ***Select, Crossover, Mutate, and Allocate*** new offspring

Use this new population for the next iteration

If the end constraint that based on the maximum fitness function realized stop, and provide the solution including the optimal values

End if

Repeat the preceding stages till reach the maximum average Dice

Record the optimal solution

iteration, where the average Dice is used as the fitness function during the GA process. The general GA procedure is introduced as follows in Algorithm 2.

This optimization process is conducted within the I–F based HBCE algorithm to determine $\beta_{\text{intensity}-optimal}$ and $\beta_{frequency-optimal}$ to guarantee the best number of clusters and their centroids within the dermoscopic images. In the training phase, the Dice metric can be defined as follows [29]:

$$Dice = \frac{2|S \cap Y|}{|S| + |Y|} \tag{14}$$

where $\cup$ refers to the union operator and $\cap$ is the intersection operator of any two sets. The Dice compares the similarity between two sets S and Y representing the segmented image and ground truth set. Thus, during the GA, the Dice is used and calculated as a fitness function, where we run the HBCE and complete all the segmentation process including using NGC within each GA iteration in the training phase till the optimal threshold values are reached, which satisfied the maximum average Dice, then the GA is stopped with reporting the values of $\beta_{\text{intensity}-optimal}$ and $\beta_{frequency-optimal}$ sequentially. These threshold optimal values after the convergence to the best Dice are then used directly in the test phase without any further GA step to determine the optimal initial number of clusters and their corresponding centroids in the NCM clustering process.

2.2. Neutrosophic graph cut

2.2.1. Neutrosophic set

Typically, the neutrosophic set (NS) deals with neutralities and their relations [30], which have a significant role in several applications to reduce the indeterminacy. Thus, in the current work, the NS based clustering is proposed to reduce the indeterminacy in the dermoscopic images for segmentation [31]. Assumes $\langle A\rangle$, $\langle Anti-A\rangle$ and $\langle Neut-A\rangle$ are an element in the NS, its opposite, its neutrality (which is neither $\langle A\rangle$nor$\langle Anti-A\rangle$). Three memberships are defined to measure the degree of truth, indeterminacy and falsity of $\langle A\rangle$, which are namely T, I, and F, respectively. These characteristics allow the neutrosophy to have an ability to measure the indeterminacy/uncertainty in the information, which is supportive to the handle the indeterminacy on skin dermoscopic images such as artifacts, noise and fuzzy edges.

2.2.2. Neutrosophic c-means clustering

The uncertain data clustering can be handled based on the NS framework for efficient clustering process using the NCM clustering process, which is formulated as a minimization problem of an objective function [32]. For each data points, the NCM computes the degrees belonging to the determinant clusters represented by T and the indeterminate clusters represented by I, and F memberships. These membership functions of the outlier and ambiguity cluster of a data point are obtained through an iterative process till it converges to a saddle point at which each data

Please cite this article as: A.R. Hawas, Y. Guo, C. Du et al., OCE-NGC: A neutrosophic graph cut algorithm using optimized clustering estimation algorithm for dermoscopic skin lesion segmentation, Applied Soft Computing Journal (2019) 105931, https://doi.org/10.1016/j.asoc.2019.105931.

point is allocated into different the cluster in consistent with the membership value [32].

In the current work, the NCM is applied to find the indeterminacy values between different intensity groups to be segmented. Each pixel $W(x, y)$ in an image is represented in the NS domain in terms of the three membership functions (MFs) as follows:

$$W_{NS}(x, y) = T(x, y), I(x, y), F(x, y) \tag{15}$$

where the $T(x, y)$, $I(x, y)$ and $F(x, y)$ denote the membership belonging to the foreground, indeterminate set, and background, respectively. Due to the fact that the objects are in the foreground, we only consider the truth T and indeterminacy I membership subsets. For a dataset $X = \{x_i, i = 1, 2, \ldots, N\}$, the true and indeterminacy membership subset values for the pixel n_i at point i are represented by $T_{NCM-n_{ij}}$ and I_{NCM-n_i}, respectively, can be expressed as follows [24]:

$$T_{NCM-n_{ij}} = \frac{Q}{w_1}(x_i - c_j)^{-\frac{2}{m-1}} \tag{16}$$

$$I_{NCM-n_i} = \frac{Q}{w_2}(x_i - \bar{c}_{i\max})^{-\frac{2}{m-1}} \tag{17}$$

where x_i represents a sample in a d-dimensional space. For C number of clusters, c_j represents the cluster centers. In the NCM, the objective function, to be minimized, depends on $Q = \left[\frac{1}{w_1}\sum_{j=1}^{C}(x_i - c_j)^{-\frac{2}{m-1}} + \frac{1}{w_2}(x_i - \bar{c}_{i\max})^{-\frac{2}{m-1}} + \frac{1}{w_3}\gamma^{-\frac{2}{m-1}}\right]^{-1}$, where w_1, w_2 and w_3 are weight factors, and γ represents a control parameter [24,32]. In addition, $\bar{c}_{i\max}$ is determined using to indexes of the largest and second-largest T_{ij} value. Since the indeterminate degree of each data depends mainly on the determinate clusters, considering the two nearest determinate clusters that have the largest and the second-largest MF values is used to reduce the computational cost (objective function) without losing efficiency [32]. Thus, at each iteration, the iterative process in the NCM is updated until the following constraint is achieved:

$$\left|T^{(k+1)}_{NCM-n_{ij}} - T^{(k)}_{NCM-n_{ij}}\right| < \ell \tag{18}$$

where ℓ is a small constant number for stopping criterion.

2.2.3. Graph cut based image segmentation

The graph theory establishes a significant framework for image segmentation. The GC, one of the most effective graph-based methods, consists of the data term that globally captures the image's characteristics in the feature space, and the smoothness term that preserves the image's spatial information [33]. The image segmentation process using GC is formulated as an energy minimization procedure [34].

Assume a graph G_{GC}, which can be represented as:

$$G_{GC} = (V_r, E_d) \tag{19}$$

where V_r is a set of vertices (pixels or regions) and E_d represents a set of edges that connect the neighboring vertices. Weight is a non-negative measure of dissimilarity which is associated with each edge using some property of the pixels. Using the GC procedure, the graph G_{GC} is divided into two subsets, namely S_c and T_c, using a cut set, which is expressed as follows:

$$C_{GC} = (S_c, T_c) = \{(u, v) \in E_d \,|u \in S_c,\ v \in T_c\} \tag{20}$$

This cut set consists of edges between the endpoints in S_c and T_c. These graph cut formulates the segmentation process as an energy minimization procedure, which in turn is converted into a minimal cut of the graph or a maximum flow problem in the graph. For a map m that assigns pixels into different clusters, the two components of the energy function E_{func} include the data term E_{data} and the smoothness term $E_{smoothness}$, where E_{data} measures the difference between m and the assigned region, and $E_{smoothness}$ evaluates the smoothness. The energy function can be represented as follows:

$$E_{func}(m) = E_{data}(m) + E_{smoothness}(m) \tag{21}$$

Generally, in order to implement the energy function, several models can be applied. In the present work, the Potts model of the energy function is used, which expressed as follows for the pixels p and q [24]:

$$E_{func}(m) = \sum_{p\in P} D_p(m_p) + \sum_{\{p,q\}\in N} V_{\{p,q\}}\left(m_p, m_q\right) \tag{22}$$

where N is the neighborhood of the current pixel p. In addition, D_p is the data function, which is used to evaluate the segmentation for the pixel p and $V_{\{p,q\}}$ is the smoothness function. After defining the energy function, the maximum flow algorithm in the graph theory is applied to segment image.

In order to gain the benefits of both the clustering-based segmentation and the graph-based segmentation, integration of the NCM clustering method into the GC technique is used [24] to achieve fast, unsupervised, and efficient solution for the skin lesion segmentation task. The NCM is used to interpret the dermoscopic image indeterminacy values between the different clusters for final segmentation using the GC method. Consequently, the NGC is applied by redefining the GC energy function in the NS domain to segment the skin lesion from the background, where D_p and $V_{\{p,q\}}$ are redefined in terms of the NCM as follows [24]:

$$D_{p-NCM}(p) = \left|T_{NCM-n_{ij}}(p) - C_j\right| \tag{23}$$

$$V_{\{p,q\}-NCM}\left(m_p, m_q\right) = \rho\eta(m_p \neq m_q) \tag{24}$$

where the constant number ρ has a value in [0,1] and $\eta(m_p \neq m_q)$ is defined as follows:

$$\eta(m_p \neq m_q) = \begin{cases} 1 & if\ m_p \neq m_q \\ 0 & otherwise \end{cases} \tag{25}$$

Accordingly, the energy function in Eq. (20) is redefined in the NS domain as follows:

$$E_{func-NGC}(m) = \sum_{p\in P} D_{p-NCM}(m_p) + \sum_{\{p,q\}\in N} V_{\{p,q\}-NCM}\left(m_p, m_q\right) \tag{26}$$

This is used for segmenting the dermoscopic images using the proposed OCE-NGC method.

2.3. Proposed system

Consequently, in the present work, to ensure the optimal clusters number and their centroids using the HBCE algorithm, an efficient optimization GA algorithm [35] is used to determine the optimal value of $\beta_{optimal}$ ($\beta_{intensity-optimal}$ and $\beta_{frequency-optimal}$) in the HBCE algorithm. In the present work, the GA is applied to define $\beta_{optimal}$ values that guarantee the best (highest) Dice values, which is used as the fitness function during the optimization process.

The present work involves the following stages: (i) convert the colored dermoscopic image to its corresponding gray-scale image, (ii) calculate the histogram representation of image, (iii) apply the proposed optimized clustering estimation procedure on the training images dataset to determine $\beta_{intensity-optimal}$ and then $\beta_{frequency-optimal}$, and (iv) apply the obtained $\beta_{intensity-optimal}$ and $\beta_{frequency-optimal}$ on the dermoscopic images to determine the optimal number of clusters and their centroids in each image of further use in the NGC algorithm for skin lesion segmentation. The proposed OCE-NGC approach is summarized in Algorithm 3 as follows.

Please cite this article as: A.R. Hawas, Y. Guo, C. Du et al., OCE-NGC: A neutrosophic graph cut algorithm using optimized clustering estimation algorithm for dermoscopic skin lesion segmentation, Applied Soft Computing Journal (2019) 105931, https://doi.org/10.1016/j.asoc.2019.105931.

Algorithm 3: Proposed OCE-NGC

Start

Transform the colored dermoscopic images to gray-scale images
Generate the histogram of each images
Identify the peak and pit points in histogram using the $I-F$ procedure
Set the initial range of $\beta_{\text{int}ensity}$ and $\beta_{frequency}$ for intensity-search and the frequency-search procedures, respectively
Set the boundary range of $\beta_{\text{int}ensity}$ and $\beta_{frequency}$ in the intensity-search and the frequency-search procedures.

Training phase of the Optimized HBCE:

Start 1

Use random values of $\beta_{\text{int}ensity}$ and $\beta_{frequency}$ from the initial range during the two search procedures

Start 2

Examine/Search the histogram using the intensity-search procedure

Calculate the mean values of the distances between each peak and the succeeding pit in gray level domain
Calculate the threshold $Th_{\text{int}ensity}$ using $\beta_{\text{int}ensity}$
Use $Th_{\text{int}ensity}$ to provide the number of max-Min points using the following steps:
If the difference between each point and the subsequent point on the histogram at peak and pit points is above the calculated threshold
Record the maximum and minimum points
Else
Eliminate the point values, which are smaller than the calculated threshold
Endif
Conclude the maximum and minimum points places on the histogram by computing the number of pixels within each histogram level

Examine/Search the histogram using the frequency-search procedure

Calculate the mean value of the difference in number of pixel between each consequence points
Calculate the threshold $Th_{frequency}$ *using* $\beta_{frequency}$
Use the threshold $Th_{frequency}$ to provide the number of clusters and its centroids using the following steps:
If the difference between each point and the subsequent point on the histogram at peak and pit points is above the calculated threshold
Record the maximum and minimum points
Else
Eliminate the point values, which are smaller than the calculated threshold
Endif
Determine the number of clusters and their centroids

Start the NGC using the determined number of clusters and their centroids
Compute the fitness function for the current image
Repeat the previous steps from "Start2" for the training images dataset
Compute the fitness function for the training images dataset
Repeat the previous steps from "Start1" which is an iterative within GA to search for $\beta_{optimal}$ ($\beta_{\text{int}ensity}$ and $\beta_{frequency}$)
Save $\beta_{optimal}$
Stop 1

Testing phase:

Start 3

Apply *the optimized HBCE algorithm using* $\beta_{optimal}$
Calculate the optimal number of clusters and their centroids without using GA
Cluster and Segment the pixels using the NGC on the test dermoscopic image dataset by defining the cost function in then the GC and segment the dermoscopic image
Stop 3

End

3. Experimental results and discussion

The experiments were taken on a workstation with a 4-core Intel(R) Core i5-5200U 2.7-GHz CPU and 8 GB RAM. The proposed OCE-NGC system is trained and evaluated using the ISIC 2016 (International Skin Imaging Collaboration) dermoscopic skin lesion images dataset for segmentation [36]. This dataset entails 900 and 379 dermoscopic images in the training and test datasets;

Please cite this article as: A.R. Hawas, Y. Guo, C. Du et al., OCE-NGC: A neutrosophic graph cut algorithm using optimized clustering estimation algorithm for dermoscopic skin lesion segmentation, Applied Soft Computing Journal (2019) 105931, https://doi.org/10.1016/j.asoc.2019.105931.

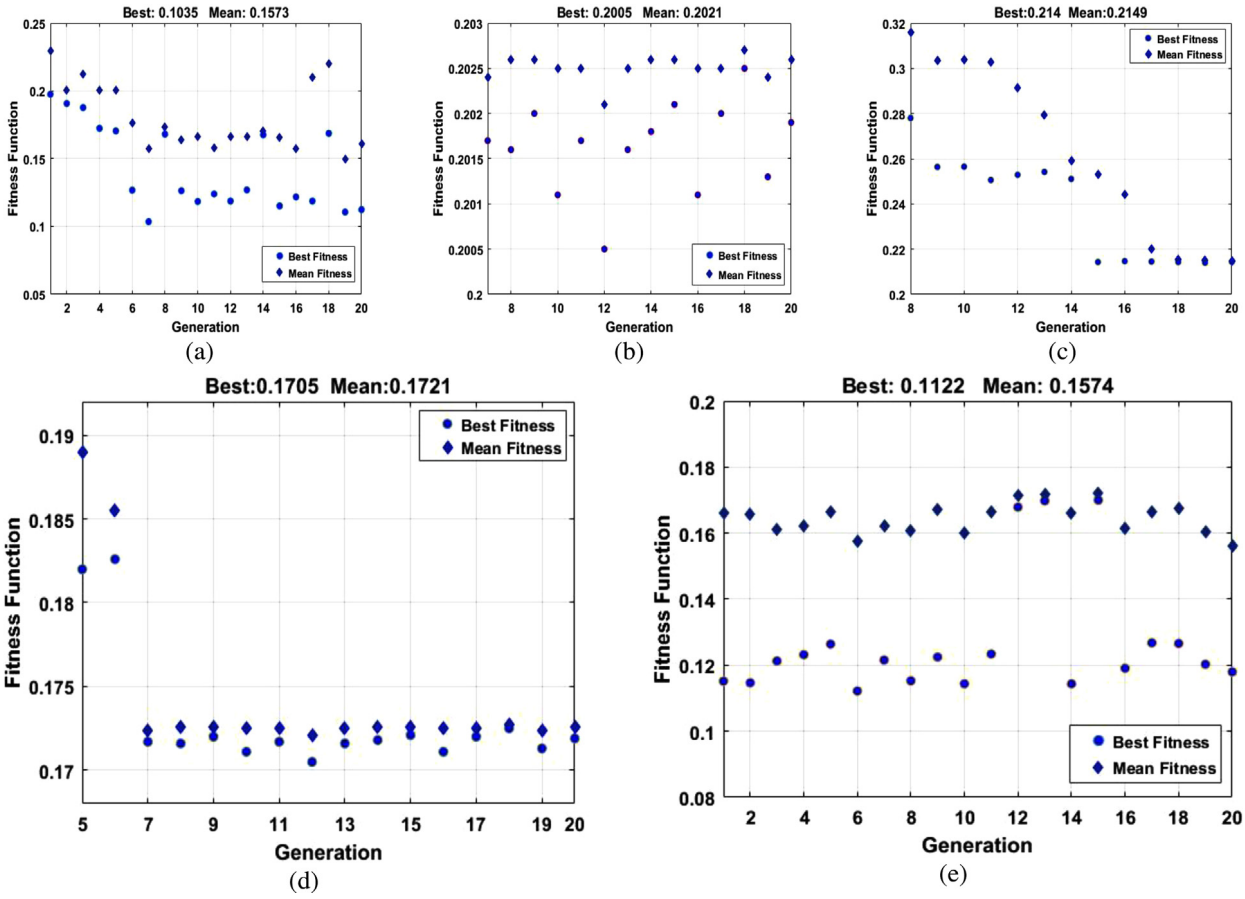

Fig. 1. Relations between the fitness function versus the generation for each iteration (cross- validation trial), where (a) through (e) represents the iteration number.

respectively with their corresponding ground truth binary images. The current work used selected images from the dataset, where the GA took time in the training phase, where the training dataset images were used to tune the proposed OCE-NGC algorithm, and the test dataset images to evaluate the performance of the proposed system by computing different metrics, namely the Jaccard index (JAC), specificity, sensitivity, and accuracy [37]. The proposed system applied the GA using the following setup parameters during the optimization process, namely population initial range from 70 to 100, 10 population size, which represents the number of iterations=10, number of generations=20, stall generation limit of 5, the average Dice as fitness function. In addition, the bounded range of $\beta_{intensity}$ is from 1 to 255, which represents the minimum and maximum of limits of any gray-scale intensity level in the histogram representation, and the bounded range of $\beta_{frequency}$ depends on the contents of the dermoscopy images. Usually, in the dermoscopy images, pixels can be assigned into skin group, lesion group and middle group. Hence, the upper bounded range of $\beta_{frequency}$ is set equal to the maximum group numbers (3). The GA is applied with cross-validation procedure for training and validation and took the average of the GA results to determine the optimized HBCE parameters, namely of the optimal $\beta_{intensity}$ and then $\beta_{frequency}$ values, which have initial values of 90, and 90, respectively in [18]. The relations between the fitness function versus the generation for each iteration are demonstrated in Fig. 1 as follows.

In addition, Table 1 reported the values of $\beta_{intensity-optimal}$ and $\beta_{frequency-optimal}$ of each iteration and their average values, which were used as the final optimal values.

Table 1
The optimal values of $\beta_{intensity}$ and $\beta_{frequency}$ at the five GA cross-validation trials (iterations).

Iteration number	$\beta_{intensity-optimal}$	$\beta_{frequency-optimal}$	Best penalty
1	221	98	0.1035
2	225	40	0.2005
3	230	110	0.214
4	239	200	0.1705
5	240	87	0.1122
Average	**231**	**107**	**0.16014**

Accordingly, in the proposed system, the obtained optimal values using the average of the five cross-validation trials (iterations) of the GA are found to be $\beta_{intensity-optimal} = 231$ and $\beta_{frequency-optimal} = 107$, which are considered the optimal values.

3.1. Intermediate results

Fig. 2 illustrates the histogram representation of an image as an example to explain the HBCE algorithm for determining the number of clusters in the image.

Fig. 2 illustrates the histogram representation of the image (ISIC_0007760) with zooming on the most significant part of the image's histogram. Typically, this image includes four clusters, where Fig. 2(a) demonstrates the image histogram for gray-scale image [0:255] level. Fig. 2(b) displays the detected maximum and minimum points form gray level [70:170] for visualization. Then, Fig. 2(c) shows a reduction in the detected peak and pit points after applying the intensity-search based procedure on the histogram. Finally, Fig. 2(d) shows the final determined number of

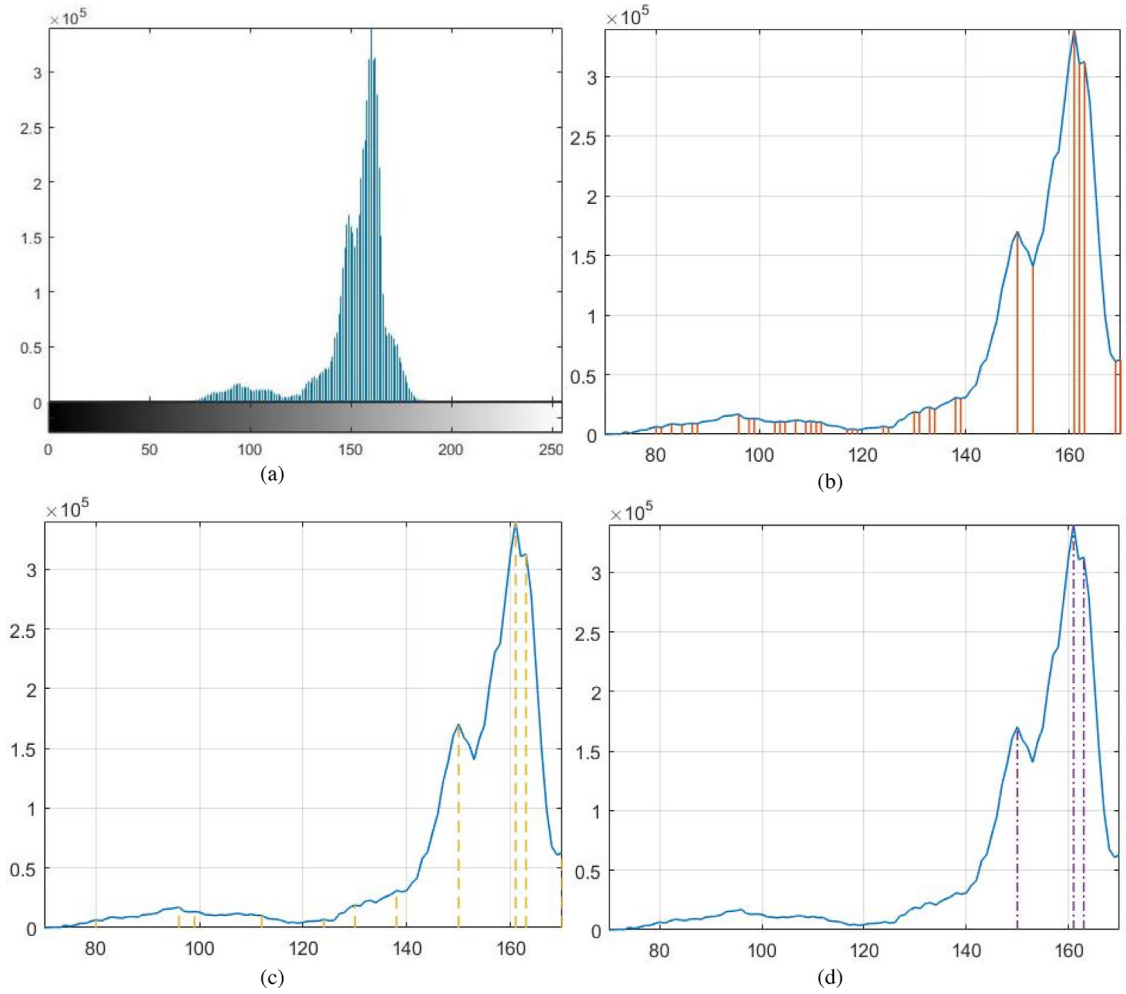

Fig. 2. Steps of the HBCE algorithm using the h-v procedure for the image ISIC_0007760.

clusters using the frequency-search based procedure on the histogram in the gray level from [70:170], which are three clusters, where the 4th cluster exists outside this displaying range. In order to illustrate the obtained results in Fig. 2 and the steps of the proposed system using the optimized HBCE with the NGC, Fig. 3 reports the NCM stages for the same image ISIC_0007760.

Fig. 3 demonstrates the proposed OCE-NGC skin lesion segmentation approach for the ISIC_0007760 image. Fig. 3 (b1–b3) illustrate the NS initial values of the membership functions of the original image. These membership functions are the true *T*, indeterminate *I*, and false *F* memberships, which refer to the degree to the determinant clusters, the degree to the boundary of clusters, and the degree belonging to the noisy dataset, respectively. Since the NCM includes an iterative process, Fig. 3(c) illustrates the last iterations, where (c1) indicates the last iteration of the NCM including the true membership function showing the four clusters, where the final NCM output is illustrated in Fig. 3(d), and the final output of the proposed system is demonstrated in Fig. 3(e) showing four main gray levels that indicate the four clusters in the image.

3.2. Comparison segmentation results

The results of the skin lesion detection by the proposed OCE-NGC system are compared to the detection results using the GC, the HBCENCM, HBCENCMGC algorithms of the dermoscopic images are illustrated in Fig. 4, where the identified boundaries are outlined in blue, while the ground truth are in red.

Fig. 4 illustrates that the detected boundaries using the proposed OCE-NGC approach are the most matched with the ground truth results compared to the other reported algorithms even with different lesion color/sizes/shapes, skin surface roughness, and light illumination. The comparison is conducted with the GC algorithm only, the NCM clustering algorithm with pre-estimation of the number of clusters, NCM clustering algorithm integrated with the GC with pre-estimation of the number of clusters, and the proposed OCE-NGC. Fig. 4 establishes the superiority of the proposed OCE-NGC method, where the segmented images (blue contours) using the proposed method achieved the best match with the ground truth (red contour) compared to the other used methods in the figure. This is due to the optimal determination of the initial clusters' numbers and corresponding centroids. However, the typical GC provided the worst results with the mismatching results of the segmented images and the corresponding ground truth results owing to the need to reduce the uncertainty in the dermoscopic images.

3.3. Performance evaluation

Several performance metrics are calculated to evaluate the proposed OCE-NGC approach in comparison to their values using the other typical segmentation algorithms. These metrics are the accuracy, Jaccard index (JAC), sensitivity, specificity, and the receiver operating characteristic (ROC) curve. Hence, Table 2 is illustrated to show the impact of using the optimized HBCE in the proposed approach to determine the initial number of

Please cite this article as: A.R. Hawas, Y. Guo, C. Du et al., OCE-NGC: A neutrosophic graph cut algorithm using optimized clustering estimation algorithm for dermoscopic skin lesion segmentation, Applied Soft Computing Journal (2019) 105931, https://doi.org/10.1016/j.asoc.2019.105931.

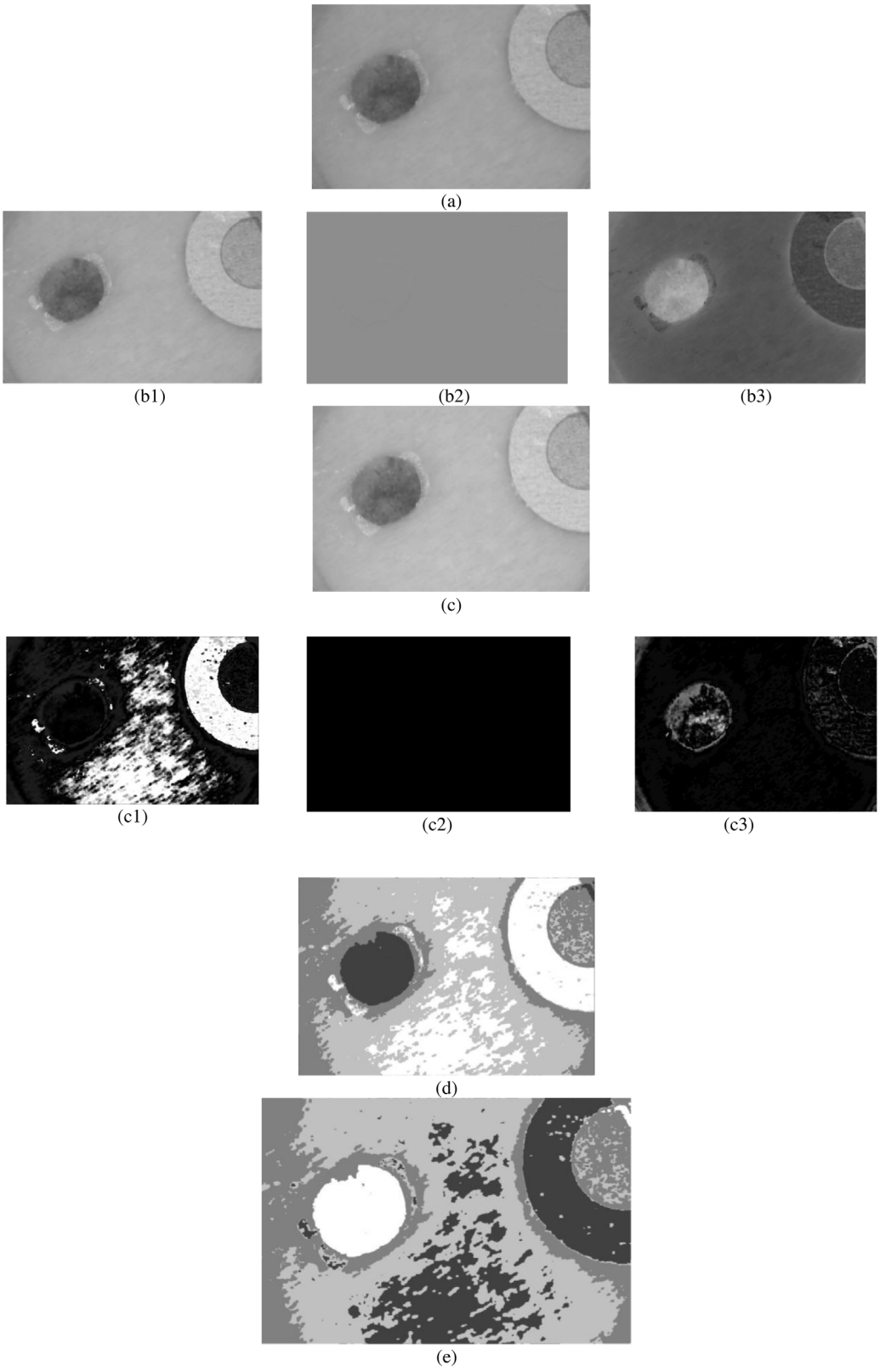

Fig. 3. NGC including NCM stages for image the ISIC_0007760: (a) Original Image in gray scale; (b1–b3) the neutrosophic memberships of the image including (b1) initial T1, (b2) initial I1, (b3) initial F1, respectively; (c) Image after modify image with I, where (c1) Last iteration NCM T, (c2) Last iteration NCM I, (c3) Last iteration NCM F; (d) NCM output; and (e) Output of the proposed optimized HBCE with NGC.

clusters compared to using the HBCE-NCM without optimization or the HBCE-NCM-GC without optimization for 5 images as an example.

From the Table 2 it is obvious that since the HBCE is performed initially prior to any further processes, thus, both using the HBCE-NCM and HBCE-NCM-GC provided the same initial number of

Please cite this article as: A.R. Hawas, Y. Guo, C. Du et al., OCE-NGC: A neutrosophic graph cut algorithm using optimized clustering estimation algorithm for dermoscopic skin lesion segmentation, Applied Soft Computing Journal (2019) 105931, https://doi.org/10.1016/j.asoc.2019.105931.

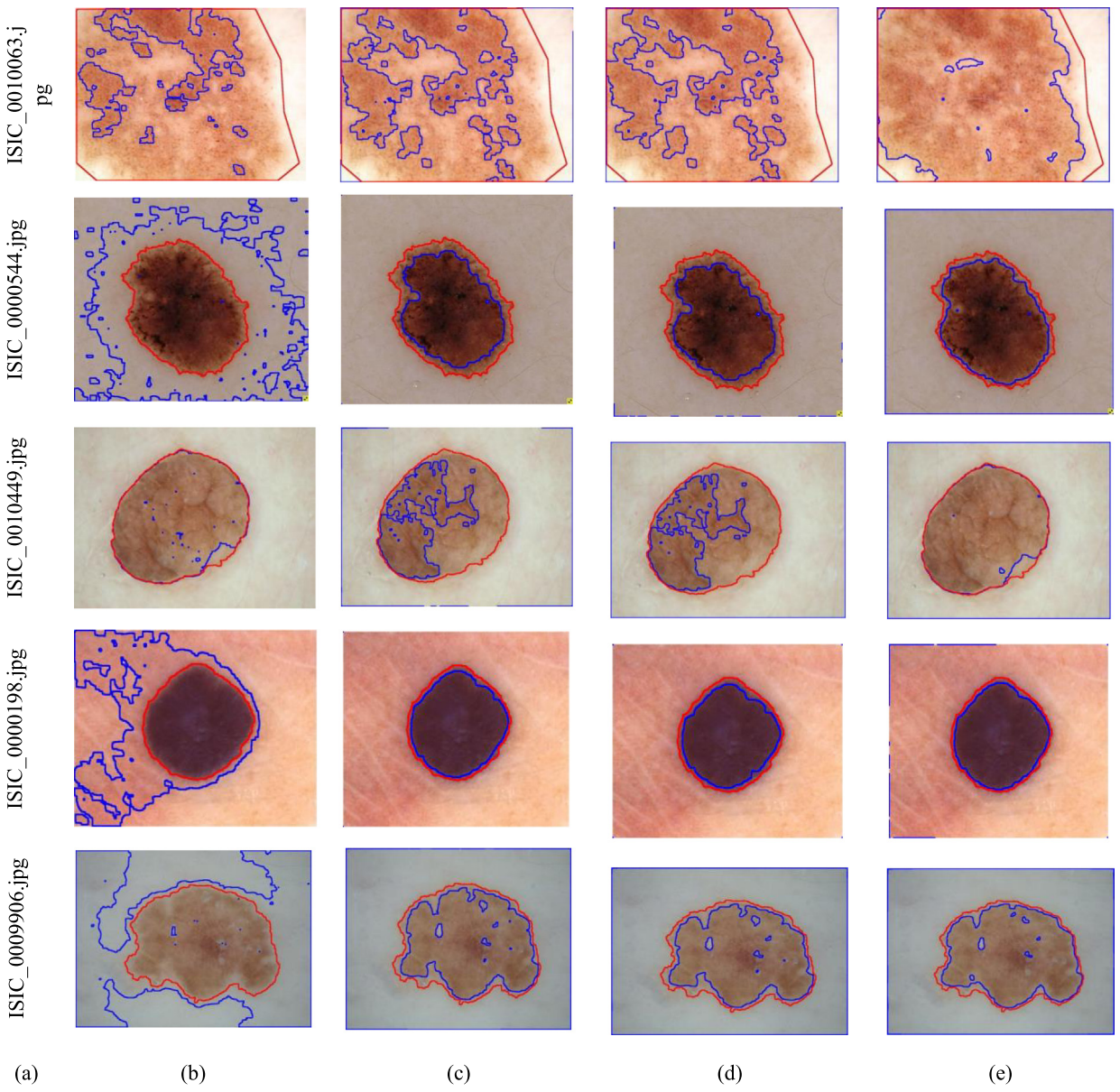

Fig. 4. The comparative segmentation results of the proposed OCE-NGC: (a) Dermoscopic image number in the test dataset of the ISIC 2016, (b–e) the detected lesion region using the GC only, the HBCENCM only, the HBCENCMGC, and the proposed Optimized HBCENCMGC (OCE-NGC); respectively.

Table 2
Example of the determined number of clusters using HBCE-NCM, HBCE-NCM-GC, and the proposed OCE-NGC.

Image ID	Number of clusters using HBCE-NCM/corresponding JAC		Number of clusters using HBCE-NCM-GC/corresponding JAC		Number of clusters using proposed OCE-NGC (optimal number of clusters)/corresponding JAC	
	K	JAC	K	JAC	K	JAC
ISIC_0000145.jpg	5	0.53	5	0.53	2	0.96
ISIC_0000029.jpg	6	0.43	6	0.44	2	0.93
ISIC_0000185.jpg	4	0.52	4	0.50	3	0.92
ISIC_0010202.jpg	4	0.41	4	0.41	2	0.89
ISIC_0000198.jpg	6	0.86	6	0.86	5	0.88

clusters 'k' for the same image. However, using the proposed optimized HBCE in the proposed OCE-NGC method provided the optimal number of clusters which is different and provided the best JAC (as reported in Table 2) as well as the other evaluation metrics. In addition, Fig. 5(a) illustrates the determined number of clusters '*k*' using the methods in Table 2 for 15 images, where their corresponding JAC values are displayed in Fig. 5(b).

Fig. 5 along with Table 2 establish the impact of the proposed optimized HBCE in determining the optimal number of clusters which is less than the determined number using HBCE-NCM or HBCE-NCM-GC without optimization. This led to a significant improvement in the performance of the segmentation method using the proposed OCE-NGC approach. Furthermore, the average values of the performance metrics over the used dataset are reported in Table 3. Table 3 illustrates the percentage values of

Please cite this article as: A.R. Hawas, Y. Guo, C. Du et al., OCE-NGC: A neutrosophic graph cut algorithm using optimized clustering estimation algorithm for dermoscopic skin lesion segmentation, Applied Soft Computing Journal (2019) 105931, https://doi.org/10.1016/j.asoc.2019.105931.

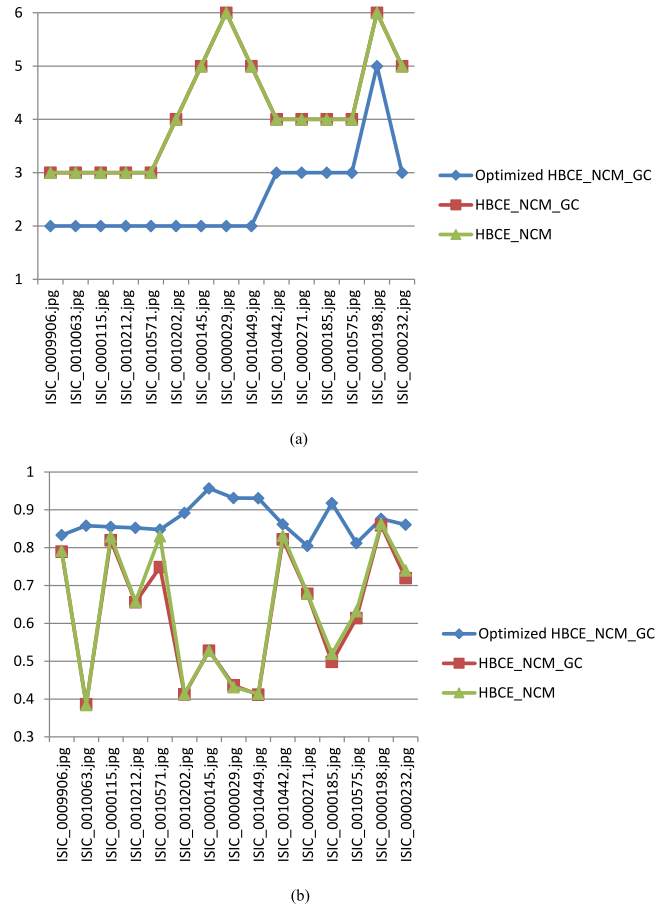

Fig. 5. Comparative study between HBCE-NCM, HBCE-NCM-GC, the optimized HBCE in the proposed OCE-NGC over 15 images in terms of (a) determined number of clusters 'k', and (b) the corresponding JAC for each segmented image.

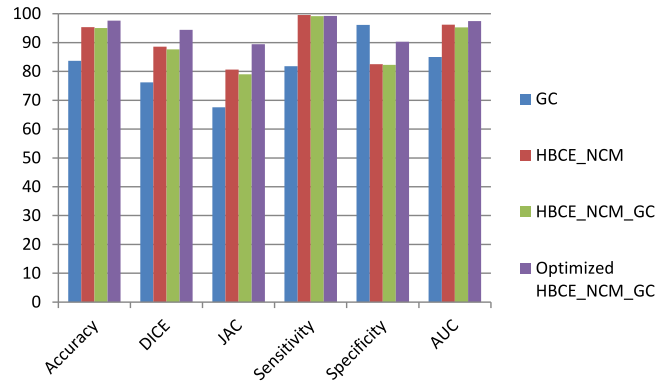

Fig. 6. The comparative evaluation metrics compared to the proposed OCE-NGC approach.

the mentioned metrics to evaluate the used algorithms in the current work in comparison with the proposed OCE-NGC system.

The comparative performance evaluation values of the different metrics in Table 3 are also illustrated in Fig. 6.

Table 3 and Fig. 6 depict the superiority of the proposed approach to segment the skin lesion regions with 97.61% accuracy value compared to the ground truth of the dermoscopic images using the h-v procedure in the optimized HBCE algorithm. It establishes that the OCE-NGC approach achieves superior accuracy, Dice, JAC, specificity and sensitivity values. In addition, accompanied by these metrics, the cumulative percentage (CP)

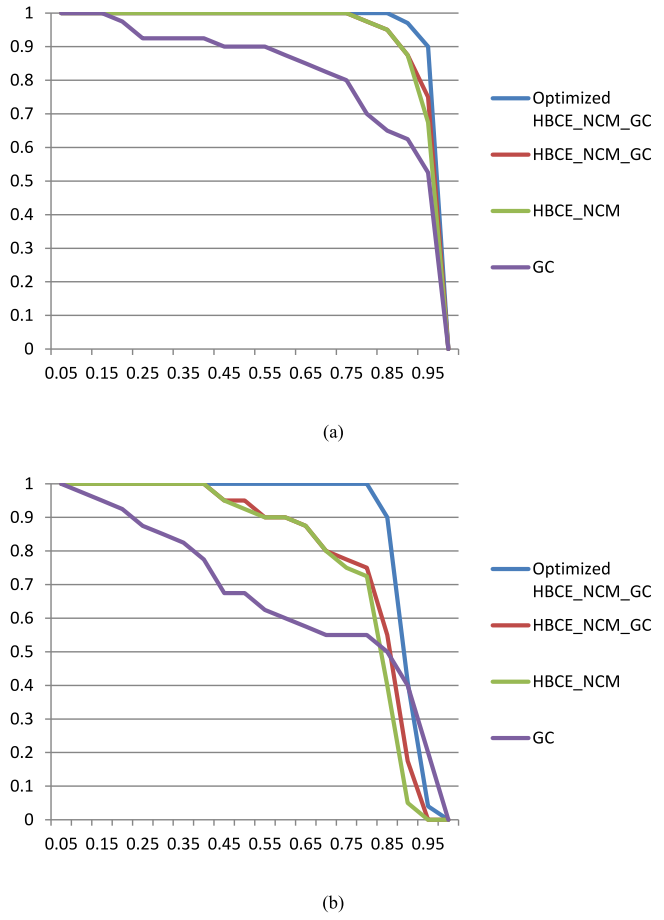

Fig. 7. Comparative CP curves, where (a) accuracy, and (b) JAC.

plot showing the percentage of the number of images that have the indicated metric value in each plot and their consistent metric values are signified on the *Y*-axis and *X*-axis, respectively. Fig. 7 includes a comparative study between the different algorithms included in the present work compared to the proposed system in terms of the CP curves of the accuracy, and the JAC performance metrics.

Fig. 7 establishes the superiority of the proposed skin lesion segmentation system based on optimized HBCE using the GA with the integrated NCM within the GC (NGC). Fig. 7(a) reports that about 98% of the images using the proposed method have about 98% maximum cumulative accuracy values. Furthermore, it shows about 85% of the images achieve about 100% JAC values. Furthermore, Fig. 8 demonstrates failed segmentation cases using the proposed method and the other methods as well.

Nevertheless, some failed cases using the proposed system occurred as demonstrated in Fig. 8. It demonstrates that the proposed approach failed to identify these lesion regions properly on the images with the lesion regions having multi-colors within the same lesion. Generally, the preceding results prove the superiority of the proposed approach with 97.61% accuracy.

4. Conclusion and future directions

Early detection of the skin lesion using the investigation and analysis of the dermoscopic images has a great impact on the accurate diagnosis and treatment. This inspired researchers to develop new segmentation techniques, which necessitates the proper determination of the number of clusters and their centroids when using the unsupervised clustering techniques for

Please cite this article as: A.R. Hawas, Y. Guo, C. Du et al., OCE-NGC: A neutrosophic graph cut algorithm using optimized clustering estimation algorithm for dermoscopic skin lesion segmentation, Applied Soft Computing Journal (2019) 105931, https://doi.org/10.1016/j.asoc.2019.105931.

Table 3
The average mean ± SD of the performance metrics of the proposed OCE-NGC approach with reference to ground truth boundaries in comparison with the typical algorithms.

Segmentation method	Accuracy (%)	Dice (%)	JAC (%)	Sensitivity (%)	Specificity (%)
GC	83.66 ± 23.24	76.21 ± 25.43	67.53 ± 30.12	81.8 ± 28.09	96.1 ± 10.46
HBCE_NCM [18]	95.37 ± 4.78	88.6 ± 9.55	80.65 ± 13.46	99.51 ± 0.57	82.53 ± 14.32
HBCE_NCM_GC	95.03 ± 4.72	87.63 ± 9.31	79.02 ± 12.95	99.16 ± 0.57	82.3 ± 14.42
Proposed OCE-NGC (Optimized HBCE h-v procedure)	97.61 ± 1.17	94.39 ± 2.08	89.44 ± 3.65	99.23 ± 0.5	97.47 ± 3.71

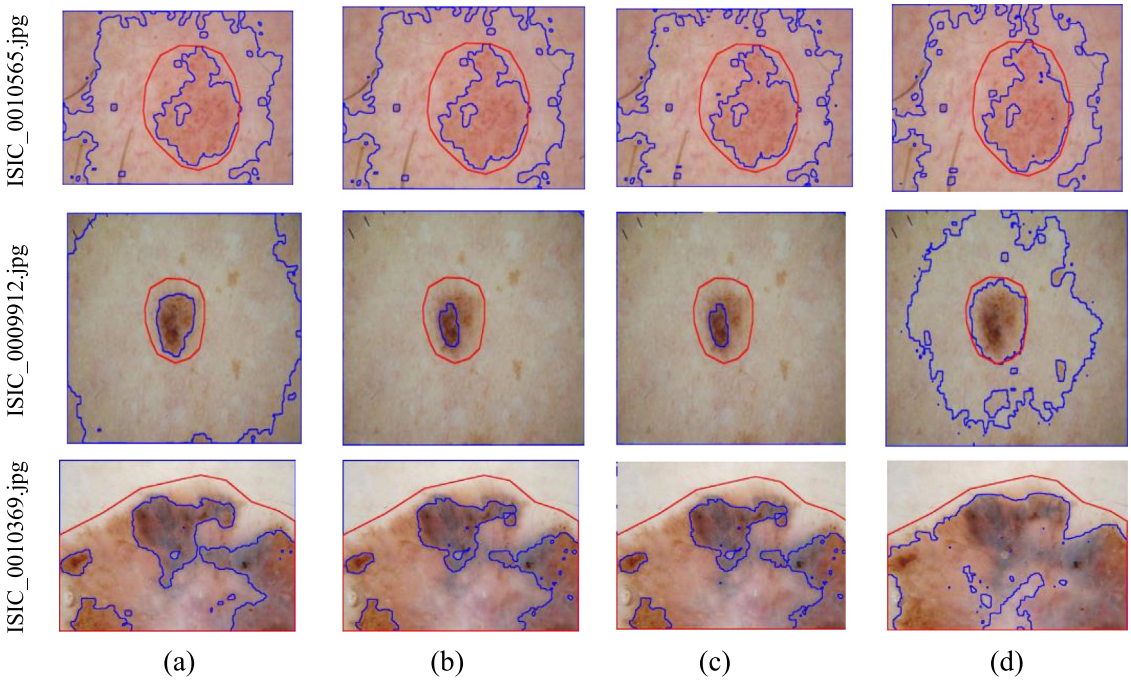

Fig. 8. Failed segmentation cases samples using (a) the proposed optimized HBCE with NGC, (b) the HBCE without optimization with the NGC, (c) the HBCE without optimization with the NCM, and (d) the typical GC without HBCE or NCM.

segmentation. Consequently, the proposed OCE-NGC approach screens the histogram of the dermoscopic images to define the optimal number of clusters for further segmentation procedure. Afterward, the optimal number of clusters is used in the neutrosophic c-means (NCM) which integrated internally in the GC forming the NGC approach. The ISIC 2016 dataset is used to train and test the proposed approach for evaluating its performance and comparing different approaches. The experimental results proved the superiority of the proposed approach for detecting the skin lesion with average accuracy of 97.61% and average JAC values of 89.44% even with uniformity dermoscopic images of different lesion shape and size. Future work will be taken on the failed cases which included multi-colors within the same lesion regions by considering using colored histogram. Furthermore, it is recommended to apply other optimization algorithms that achieved superior performance in different applications as in [38–45].

Declaration of competing interest

No author associated with this paper has disclosed any potential or pertinent conflicts which may be perceived to have impending conflict with this work. For full disclosure statements refer to https://doi.org/10.1016/j.asoc.2019.105931.

References

[1] R. Sumithra, M. Suhil, D.S. Guru, Segmentation and classification of skin lesions for disease diagnosis, Procedia Comput. Sci. 45 (2015) 76–85.

[2] M.I. Rajab, M.S. Woolfson, S.P. Morgan, Application of region-based segmentation and neural network edge detection to skin lesions, Comput. Med. Imaging Graph. 28 (1–2) (2004) 61–68.

[3] H. Wang, R.H. Moss, X. Chen, R.J. Stanley, W.V. Stoecker, M.E. Celebi, …, S.W. Menzies, Modified watershed technique and post-processing for segmentation of skin lesions in dermoscopy images, Comput. Med. Imaging Graph. 35 (2) (2011) 116–120.

[4] M. Ménard, C. Demko, P. Loonis, The fuzzy c+ 2-means: solving the ambiguity rejection in clustering, Pattern Recognit. 33 (7) (2000) 1219–1237.

[5] J.C. Bezdek, J. Keller, R. Krisnapuram, N. Pal, Fuzzy Models and Algorithms for Pattern Recognition and Image Processing (Vol. 4), Springer Science & Business Media, 2006.

[6] A. Baraldi, P. Blonda, A survey of fuzzy clustering algorithms for pattern recognition I, IEEE Trans. Syst. Man Cybern. B 29 (6) (1999) 778–785.

[7] T. Zhao, A. Nehorai, B. Porat, K-means clustering-based data detection and symbol-timing recovery for burst-mode optical receiver, IEEE Trans. Commun. 54 (8) (2006) 1492–1501.

[8] J. Kang, L. Min, Q. Luan, X. Li, J. Liu, Novel modified fuzzy c-means algorithm with applications, Digit. Signal Process. 19 (2) (2009) 309–319.

[9] H. Zhou, G. Schaefer, A.H. Sadka, M.E. Celebi, Anisotropic mean shift based fuzzy c-means segmentation of dermoscopy images, IEEE J. Sel. Top. Sign. Proces. 3 (1) (2009) 26–34.

[10] H. Lee, Y.P.P. Chen, Skin cancer extraction with optimum fuzzy thresholding technique, Appl. Intell. 40 (3) (2014) 415–426.

[11] D.L. Pham, Spatial models for fuzzy clustering, Comput. Vis. Image Underst. 84 (2) (2001) 285–297.

[12] Y. Guo, A.S. Ashour, F. Smarandache, A novel skin lesion detection approach using neutrosophic clustering and adaptive region growing in dermoscopy images, Symmetry 10 (4) (2018) 119.

[13] A.S. Ashour, A.R. Hawas, Y. Guo, M.A. Wahba, A novel optimized neutrosophic k-means using genetic algorithm for skin lesion detection in dermoscopy images, Signal Image Video Process. (2018) 1–8.

[14] H.P. Chen, X.J. Shen, J.W. Long, Histogram-based colour image fuzzy clustering algorithm, Multimedia Tools Appl. 75 (18) (2016) 11417–11432.

[15] J. Pei, L. Zhao, X. Dong, X. Dong, Effective algorithm for determining the number of clusters and its application in image segmentation, Cluster Comput. 20 (4) (2017) 2845–2854.
[16] E. Küçükkülahlı, P. Erdoğmuş, K. Polat, Histogram-based automatic segmentation of images, Neural Comput. Appl. 27 (5) (2016) 1445–1450.
[17] K.S. Tan, N.A.M. Isa, Color image segmentation using histogram thresholding–Fuzzy C-means hybrid approach, Pattern Recognit. 44 (1) (2011) 1–15.
[18] A.S. Ashour, Y. Guo, E. Kucukkulahli, P. Erdogmus, K. Polat, A hybrid dermoscopy images segmentation approach based on neutrosophic clustering and histogram estimation, Appl. Soft Comput. 42 (2018) 6–434.
[19] N.R. Pal, S.K. Pal, A review on image segmentation techniques, Pattern Recognit. 26 (9) (1993) 1277–1294.
[20] P.F. Felzenszwalb, D.P. Huttenlocher, Efficient graph-based image segmentation, Int. J. Comput. Vis. 59 (2) (2004) 167–181.
[21] O. Lézoray, M. Revenu, M. Desvignes, Graph-based skin lesion segmentation of multispectral dermoscopic images, in: Image Processing, ICIP, 2014 IEEE International Conference on, IEEE, 2014, pp. 897–901.
[22] E.S. Flores, J. Scharcanski, Segmentation of pigmented melanocytic skin lesions based on learned dictionaries and normalized graph cuts, in: Graphics, Patterns and Images, SIBGRAPI, 2014 27th SIBGRAPI Conference on, IEEE, 2014, pp. 33–40.
[23] R. Kéchichian, H. Gong, M. Revenu, O. Lézoray, M. Desvignes, New data model for graph-cut segmentation: application to automatic melanoma delineation, in: Image Processing, ICIP, 2014 IEEE International Conference on, IEEE, 2014, pp. 892–896.
[24] Y. Guo, Y. Akbulut, A. Şengür, R. Xia, F. Smarandache, An efficient image segmentation algorithm using neutrosophic graph cut, Symmetry 9 (9) (2017) 185.
[25] E. Abdel-Maksoud, M. Elmogy, R. Al-Awadi, Brain tumor segmentation based on a hybrid clustering technique, Egypt. Inform. J. 16 (1) (2015) 71–81.
[26] R.S. Perumal, P.V.S.S.R. Chandra Mouli, An efficient color image segmentation algorithm using hybrid approaches, in: Proceedings of the Seventh Indian Conference on Computer Vision, Graphics and Image Processing, ACM, 2010, pp. 435–439.
[27] M. Mignotte, Segmentation by fusion of histogram-based k-means clusters in different color spaces, IEEE Trans. Image Process. 17 (5) (2008) 780–787.
[28] D. Hao, Q. Li, C. Li, Histogram-based image segmentation using variational mode decomposition and correlation coefficients, Signal Image Video Process. 11 (8) (2017) 1411–1418.
[29] L. Rundo, C. Militello, G. Russo, A. Garufi, S. Vitabile, M.C. Gilardi, G. Mauri, Automated prostate gland segmentation based on an unsupervised fuzzy C-means clustering technique using multispectral T1w and T2w MR imaging, Information 8 (2) (2017) 49.
[30] F. Smarandache (Ed.), A unifying field in logics: Neutrosophic logic. neutrosophy, neutrosophic set, neutrosophic probability: Neutrosophic logic: Neutrosophy, neutrosophic set, neutrosophic probability. Infinite study, 2003.
[31] Y. Guo, R. Xia, A. Şengür, K. Polat, A novel image segmentation approach based on neutrosophic c-means clustering and indeterminacy filtering, Neural Comput. Appl. 28 (10) (2017) 3009–3019.
[32] Y. Guo, A. Sengur, NCM: Neutrosophic c-means clustering algorithm, Pattern Recognit. 48 (8) (2015) 2710–2724.
[33] M.J. Kumar, D.G.R. Kumar, R.V.K. Reddy, Review on image segmentation techniques, Int. J. Sci. Res. Eng. Technol. (2014).
[34] Y. Boykov, O. Veksler, R. Zabih, Fast approximate energy minimization via graph cuts, IEEE Trans. Pattern Anal. Mach. Intell. 23 (11) (2001) 1222–1239.
[35] J.P. Li, M.E. Balazs, G.T. Parks, Engineering design optimization using species-conserving genetic algorithms, Eng. Optim. 39 (2) (2007) 147–161.
[36] Imaging Collaboration, International Skin Website. http://www.isdis.net/index.php/isic-project.
[37] Y. Guo, C. Zhou, H.P. Chan, A. Chughtai, J. Wei, L.M. Hadjiiski, E.A. Kazerooni, Automated iterative neutrosophic lung segmentation for image analysis in thoracic computed tomography, Med. Phys. 40 (8) (2013).
[38] H. Xing, X. Zhou, X. Wang, S. Luo, P. Dai, K. Li, H. Yang, An integer encoding grey wolf optimizer for virtual network function placement, Appl. Soft Comput. 76 (2019) 575–594.
[39] M. Mafarja, I. Aljarah, A.A. Heidari, H. Faris, P. Fournier-Viger, X. Li, S. Mirjalili, Binary dragonfly optimization for feature selection using time-varying transfer functions, Knowl.-Based Syst. 161 (2018) 185–204.
[40] H. Faris, M.M. Mafarja, A.A. Heidari, I. Aljarah, .A.Z. Ala', S. Mirjalili, H. Fujita, An efficient binary salp swarm algorithm with crossover scheme for feature selection problems, Knowl.-Based Syst. 154 (2018) 43–67.
[41] M. Mafarja, I. Aljarah, A.A. Heidari, H. Faris, P. Fournier-Viger, X. Li, S. Mirjalili, Binary dragonfly optimization for feature selection using time-varying transfer functions, Knowl.-Based Syst. 161 (2018) 185–204.
[42] I. Aljarah, M. Mafarja, A.A. Heidari, H. Faris, Y. Zhang, S. Mirjalili, Asynchronous accelerating multi-leader salp chains for feature selection, Appl. Soft Comput. 71 (2018) 964–979.
[43] A.A. Heidari, P. Pahlavani, An efficient modified grey wolf optimizer with Lévy flight for optimization tasks, Appl. Soft Comput. 60 (2017) 115–134.
[44] M.A. Al-Betar, M.A. Awadallah, H. Faris, I. Aljarah, A.I. Hammouri, Natural selection methods for grey wolf optimizer, Expert Syst. Appl. 113 (2018) 481–498.
[45] A.A. Heidari, I. Aljarah, H. Faris, H. Chen, J. Luo, S. Mirjalili, An enhanced associative learning-based exploratory whale optimizer for global optimization, Neural Comput. Appl. (2019) 1–27.

Please cite this article as: A.R. Hawas, Y. Guo, C. Du et al., OCE-NGC: A neutrosophic graph cut algorithm using optimized clustering estimation algorithm for dermoscopic skin lesion segmentation, Applied Soft Computing Journal (2019) 105931, https://doi.org/10.1016/j.asoc.2019.105931.